SERI/TP-217-3276
UC Category: 60
DE88001123

Preliminary Results from the Dynamic Response Testing of the Westinghouse 600-kW Wind Turbine

S.M. Hock
T.E. Hausfeld
R.W. Thresher

December 1987

Prepared for Windpower '87
San Francisco, California
5-8 October, 1987

Prepared under Task No. WE721202

Solar Energy Research Institute
A Division of Midwest Research Institute

1617 Cole Boulevard
Golden, Colorado 80401-3393

Prepared for the
U.S. Department of Energy
Contract No. DE-AC02-83CH10093

Printed in the United States of America
Available from:
National Technical Information Service
U.S. Department of Commerce
5285 Port Royal Road
Springfield, VA 22161

Price: Microfiche A01
Printed Copy A02

Codes are used for pricing all publications. The code is determined by the number of pages in the publication. Information pertaining to the pricing codes can be found in the current issue of the following publications, which are generally available in most libraries: *Energy Research Abstracts, (ERA); Government Reports Announcements* and Index (*GRA* and I); *Scientific and Technical Abstract Reports (STAR);* and publication, NTIS-PR-360 available from NTIS at the above address.

SERI

PRELIMINARY RESULTS FROM THE DYNAMIC RESPONSE TESTING OF THE WESTINGHOUSE 600-kW WIND TURBINE

T. E. Hausfeld
S. M. Hock
R. W. Thresher
Solar Energy Research Institute
1617 Cole Boulevard, Golden, Colo 80401

ABSTRACT

This paper provides a preliminary look at test data from a Westinghouse 600-kW wind turbine. The Westinghouse machine was fitted with instrumentation to record machine data, as well as wind and atmospheric conditions. Wind data were collected from five levels of anemometers mounted on a meteorological tower upwind of the turbine. Because of problems encountered while digitizing the data, this paper presents results from a very limited number of channels and time-series data segments. Three sets of 10-minute data segments are presented that cover power, pitch angle, and blade loads.

Because of the narrow scope of this analysis, the following conclusions should be considered tentative: (1) Energy production appears to be somewhat better than predicted. (2) The teetering hub appears to be operating as expected, and the rotor is teetering to eliminate much of the loading caused by the mean wind shear in the inflow. (3) A large part of the flapping-moment variation is caused by low-frequency turbulence in the inflow.

TURBINE DESCRIPTION

The field test turbine, manufactured by the Westinghouse Electric Corporation, was an upwind, horizontal-axis, two-bladed, teetered-hub machine with full span pitch control and a synchronous generator. It was rated at 600 kW at a hub-height wind speed of 30 mph. It was designed to begin producing power at a cut-in wind speed of 14 mph, and to shut down when wind speeds exceed 50 mph. Figure 1 (taken from [1]) shows the test machine with a hub height of 120 ft and a tubular steel tower.

The molded wood/epoxy laminate blades and the hub assembly comprised the rotor, which had a diameter

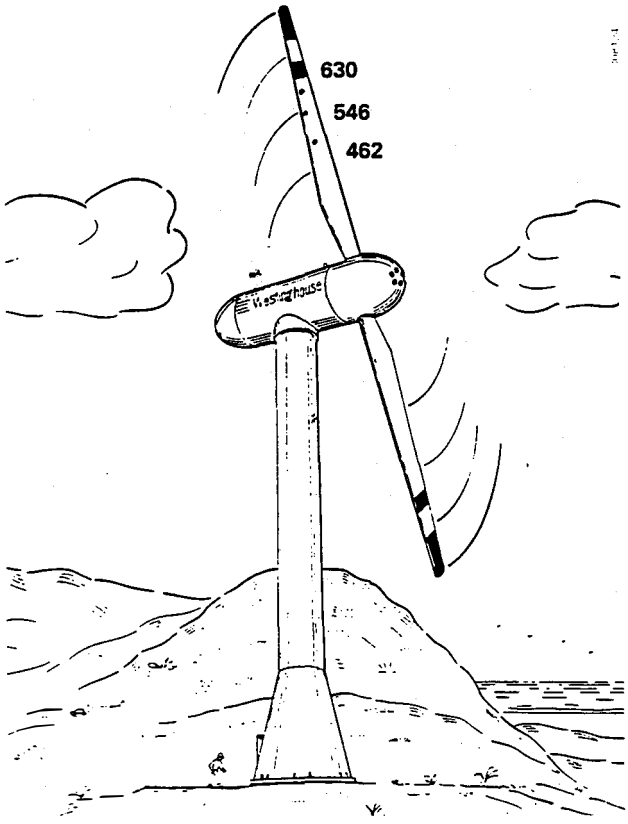

Figure 1. STRAIN-GAGE LOCATIONS ON THE WESTINGHOUSE 600-kW WIND TURBINE

of 142 ft and rotated at a constant speed of 43 rpm. The hub was mounted at a tilt angle of 4 degrees, and the blades were a modified LS(1)-04XX airfoil with a nonlinear, 6.75-degree twist and no precone angle. Table 1 summarizes the machine's characteristics.

The Westinghouse machine had a unique power control algorithm, which limited high instantaneous power spikes (caused by sudden wind gusts) by derating the maximum power level by 10% whenever a power spike exceeded 800 kW. Thus, the machine could be operated at 10%, 20%, or 30% reduced power for long periods of time.

Table 1. WIND TURBINE CHARACTERISTICS

Rated power	600 kW
Rotor diameter	43.3 m (142 ft)
Rotor orientation	Upwind
Rotor type	Teetered
Hub height	36.6 m (120 ft)
Cone angle	0 degrees
Tilt angle	4 degrees
Delta-3	0 degrees
Method of power regulation	Full span pitch control
Airfoil	Modified LS(1)-04XX
Twist	6.75 degrees (nonlinear)
Blade material	Laminated wood composite
Rotor speed	43 rpm
Generator speed	1800 rpm
Generator type	Synchronous
Low wind cut-in	6.25 m/s (14 mph)
Rated wind speed	12.8 m/s (28.6 mph)
High wind cut-out	22.3 m/s (50 mph)
Control	Microcomputer
Blade 1st cantilever bending frequency	
flapwise	2.24 Hz
chordwise	4.56 Hz

INSTRUMENTATION

The wind turbine was heavily instrumented, with 40 data channels devoted to recording machine data. An additional 23 channels were used to monitor the wind and atmospheric conditions. The combined total of 63 analog channels were FM-multiplexed and recorded on a 14-channel Sabre VI tape recorder. A summary of the channels is presented in Table 2. The analog tapes were then returned to SERI, where they were low-pass filtered and digitized on a Neff 720 system. The machine

Table 2. SUMMARY OF DATA CHANNELS

Signal number	Channel description
1-15	5 levels of UVW wind speeds
16	HERS tower anemometer
17	HERS wind direction
18,19	Horizontal and vertical hot-film wind speed
20	Temperature at top of rotor
21	Temperature difference across rotor disk
22	Barometric pressure
23	Humidity
24,25	Tower strain gages
26	Rotor azimuth position
27	DC reference signal
28	Teeter angle
29	Blade pitch angle
30	Generator power
31	Yaw angle
32-34	Blade #1 strain gages
35-37	Blade #2 strain gages
38-63	Strain gages located at high-stress locations on the rotor, bedplate, and tower

data of primary interest for this study included the rotor azimuth position, pitch angle, generator power, and the three strain gages on blade #2 (located as indicated in Figure 1).

The wind data were collected from five UVW Gill propeller anemometers located on a meteorological tower 180 feet upwind of the turbine. The five levels represent the top and bottom of the rotor, hub height, and two locations at the midspan of the blades. Located further upwind, the Hawaiian Energy Renewable Systems (HERS) meteorological tower contained a single hub-height anemometer.

In parallel with the analog data recording, a "quick look" midscale data system was employed. This system included a COMPAQ 386 personal computer using LABTECH Notebook software and Keithly data-acquisition hardware. The system was used to digitize selected channels and store the data on the

hard disk. The atmospheric data were sampled at 5 Hz, and all other channels were sampled at 30 Hz. These data were later transferred to a 1/4-in., 60-MByte streaming tape, using Kammerman hardware, for further analysis.

STUDY DATA CASES

Data were collected from the Westinghouse turbine located in the Makani Moa'e wind-farm project of HERS from March 18 through April 4, 1987. A total of 26 hours of data were recorded on the analog tapes; the data covered a wide range of environmental conditions, including low and high wind speeds, turbulence levels, wind shear, and precipitation. In addition, the wind turbine was subjected to several off-normal shut-down events to record the loads. Vortex generators (VGs) were attached to the inboard of the blade span for half of the test and to the full blade span for the other half of the test.

The analog data recorded at the site was divided into runs lasting one hour; two minutes of low and high calibrations were recorded at the beginning and end of each run. Selected channels from most of these hour-long runs were simultaneously digitized on the midscale system and stored on streaming tapes for quick-look analysis. These data form the field-digitized data set.

Upon returning the analog tapes to SERI for digitization and processing, a significant low-frequency noise signal was discovered that contaminated all of the analog data. To proceed with this preliminary presentation of test results, the field-digitized data were used since they were not affected by the noise, which was probably introduced to the analog stream in the tape recorder.

The value of the field-digitized data is limited since the data underwent no filtering (and thus contained high-frequency noise) and did not make up a complete data set. However, the data were useful for a preliminary analysis, and the data and channels were searched to find three usable data sets that covered the most important channels (including power, pitch angle, and blade loads). The strain gages were installed on the low-pressure side of the blade only, which makes the mean blade loads difficult to compute. Therefore, for this quick-look study, the mean loads were removed; the residual load characteristics are presented. Another factor that limited the selection of data cases was the amount of processing required to compute the wind speeds from the UVW Gill anemometers. This requires an iterative procedure to correct for the wind direction when it is significantly out of line with the U arm of the anemometer. Therefore, only cases with a wind direction colinear with the U arm were selected.

Given these restraints, Table 3 summarizes the three 10-min data cases that were selected. The three cases cover a range of disk-averaged wind speeds from 21 to 32 mph, turbulence intensities from 12% to 23%, half and full VGs, and 80%, 90%,

Table 3. SUMMARY DESCRIPTION OF THE QUICK-LOOK DATA CASES

Run	Date, time (24 h)	V (mph)	Turbulence Intensity	Comments
2	3/19/87, 16:17	31.7	12%	Power derated to 80%, half VGs
18	4/1/87, 10:23	29.0	23%	Power derated to 90%, full VGs
25	4/3/87, 14:29	21.5	22%	Full power, below rated operation, full VGs

and 100% power derating factors. Because of all of these operational differences between the cases, caution must be exercised in comparing the data.

The data analysis procedure used for this study is intended to provide preliminary indications of the wind turbine's operating characteristics. The data were preaveraged over one rotor revolution and then binned versus disk-averaged wind speed. We also binned the time-series data versus blade azimuth position and fit a 6th-order Fourier series to the azimuth-averaged data to provide an estimate of the deterministic signal. The residual time series of the loads (i.e., the original time series with the linear trend removed) was then transformed to the frequency domain, and power spectral density plots were presented to provide an insight into the nature of the random loads.

MEAN POWER AND PITCH ANGLE

The mean turbine power output and pitch angle were determined using the method of bins. They were preaveraged over a time period equal to one rotor revolution to average out higher harmonic responses. The wind-speed signal used to bin the responses was formed by computing a rotor-disk-averaged wind signal, given by

$$\hat{U}_{disk} = (\hat{U}_1 + \hat{U}_2 + \hat{U}_3 + \hat{U}_4 + \hat{U}_5)/5 \ ,$$

where each of the $\hat{U}_i$ wind signals was also preaveraged over a period of one rotor revolution. The power and pitch signals were binned into 1-mph wind bins, and bins containing fewer than 10 data points were discarded. No density corrections were applied for this preliminary data analysis.

Figure 2 shows the power curve obtained by this procedure for all three data cases, and it also shows the Westinghouse projected power curve. For data cases #18 and #25, VGs were installed along the entire blade length; for data case #2, VGs were installed only along the inboard half of the blade. Also for data case #2, the turbine controller was set to maintain 80% of rated power; for case #18, the controller was attempting to hold 90% of rated power. Figure 3 shows pitch angle versus wind speed for all three data cases. These plots clearly indicate the general trends versus wind speed; however, there is not enough data to provide a quantitative description of the actual behavior.

ANALYSIS OF THE BLADE'S CYCLIC LOADS

Figure 4 shows a seven-revolution time history of the flapwise bending moment for blade station 546 (65% span) for data case #25. The figure also includes the blade position signal, which is the

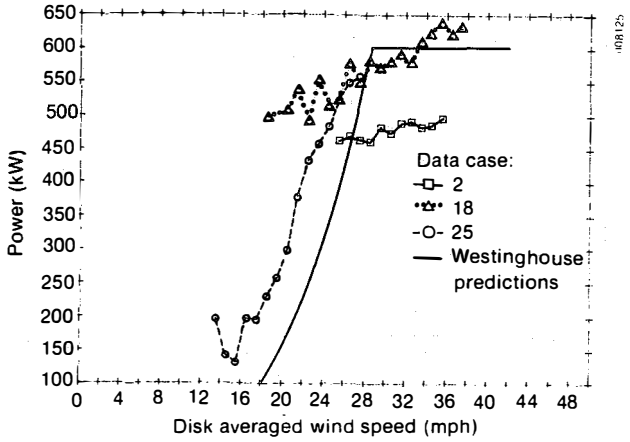

Figure 2. POWER CURVE FOR THE WESTINGHOUSE 600-kW WIND TURBINE

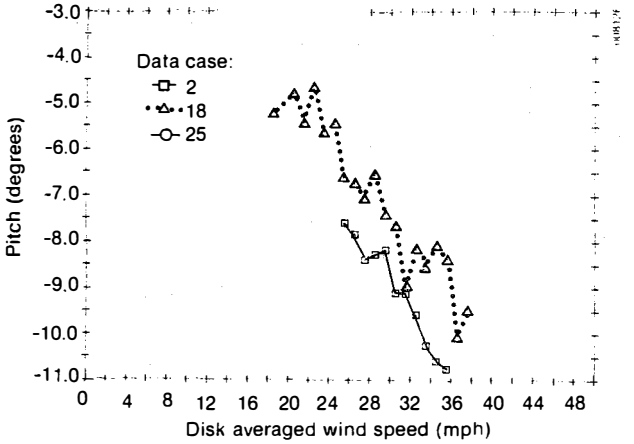

Figure 3. PITCH ANGLE VERSUS WIND SPEED FOR ALL DATA CASES

saw-tooth trace at the bottom of the plot. The mean bending moment has been removed; the figure illustrates only the cyclic fluctuations. Figure 5 is the flapwise bending moment, at the same location, 100 seconds later. Comparing Figure 5 with Figure 4 reveals the variability in the loading over relatively short time spans. In Figure 4, the bending moment is relatively low-amplitude and has considerable high-frequency content; Figure 5 shows a high-amplitude bending moment at a frequency of 2 per revolution (2P) with somewhat less high-frequency content. These time histories contain the deterministic and stochastic loads due to turbulence. The large difference between these signals suggests a rather small deterministic contribution to the cyclic loads, and also a large stochastic contribution; otherwise, the signals would be quite similar.

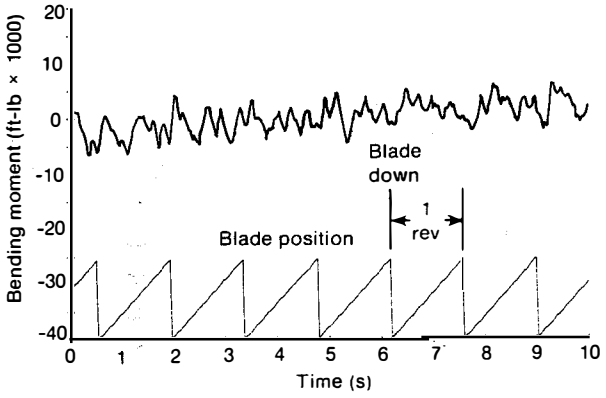

Figure 4. TIME-SERIES SEGMENT OF THE FLAPWISE BENDING MOMENT FOR BLADE STATION 546 (MEAN REMOVED AT THE START OF DATA CASE #25)

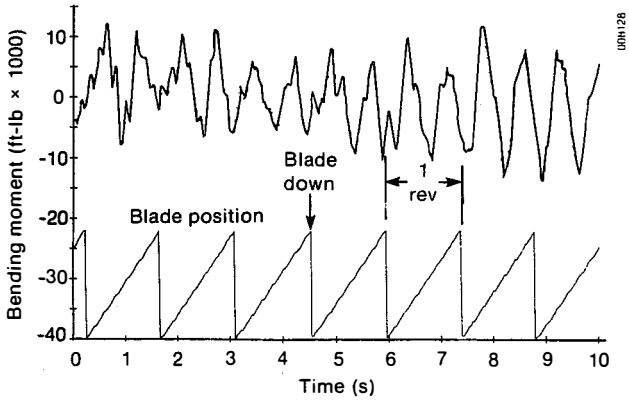

Figure 5. TIME-SERIES SEGMENT OF THE FLAPWISE BENDING MOMENT FOR BLADE STATION 546 (MEAN REMOVED AT 100 SECONDS INTO DATA CASE #25)

For data case #25, the deterministic component of the cyclic bending moment for blade station 546 was determined by azimuth averaging. Azimuth averaging is accomplished by binning the bending moment with respect to the azimuth angle of the blade for the entire 10-min data case. The results of this computation are illustrated in Figure 6, where a Force and Loads Analysis Program (FLAP) [2] dynamic-response code run is provided for comparison. The FLAP code run was made at the same mean wind speed; it uses a 1/7 power-law wind shear profile with no tower shadow. This confirms that the deterministic cyclic loads are fairly small, particularly when compared to those illustrated in Figure 5's time history. The FLAP code was run only to confirm the order of magnitude of the deterministic signal and to see if the waveforms were similar (which they are).

Auto-spectral density plots for the flapwise bending moment at station 546, for all data cases, are shown in Figures 7, 8 and 9, respectively. It is misleading to make much of a comparison between the plots because the turbine was operated in a different mode for each case. Case #2 had VGs installed on half of the blade with the controller set to maintain 80% of rated power, while for

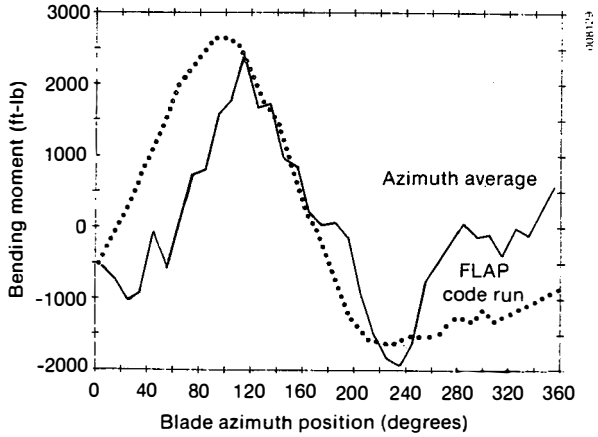

Figure 6. AZIMUTH-AVERAGED FLAPWISE BENDING MOMENT FOR STATION 546 WITH MEAN REMOVED, AND FLAP DYNAMICS CODE COMPARISON RUN

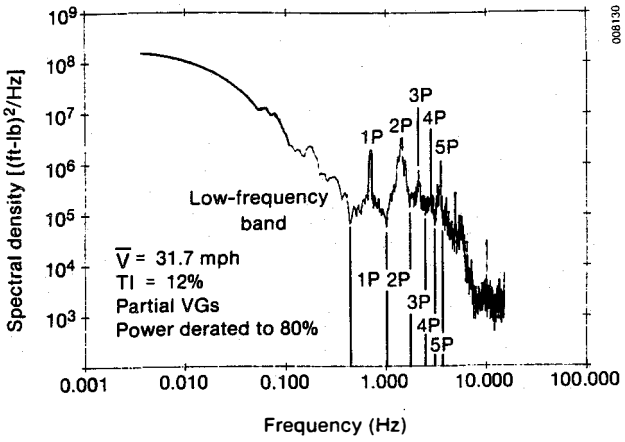

Figure 7. SPECTRAL DENSITY OF THE STATION 546 FLAPWISE BENDING MOMENT FOR DATA CASE #2

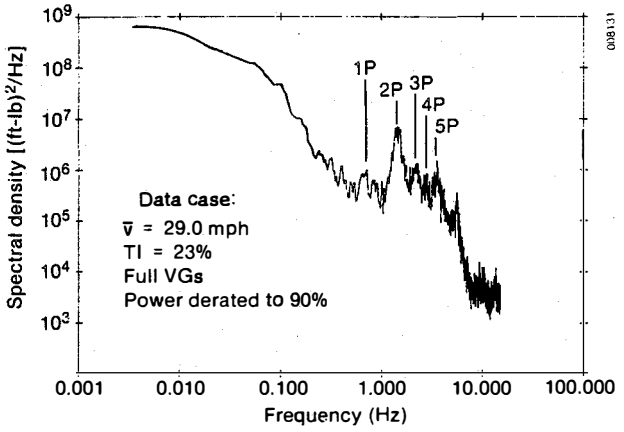

Figure 8. SPECTRAL DENSITY OF THE STATION 546 FLAPWISE BENDING MOMENT FOR DATA CASE #18

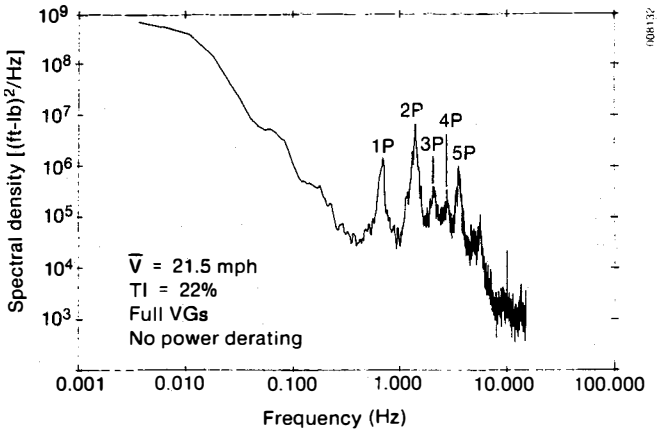

Figure 9. SPECTRAL DENSITY OF THE STATION 546 FLAPWISE BENDING MOMENT FOR DATA CASE #25

case #18 the controller was set for 90% of rated power. Case #25 was far below the rated wind speed. In spite of these differences, there are some striking similarities. All of the spectral plots show well-defined spikes at multiples of the rotor passage frequency, out to 5P. This would tend to indicate a rather complex mean inflow wind profile, or possibly that one of the blades has slightly different aerodynamic properties. In addition, the spectral density in the region below 1P is considerably higher than even the peaks of the spikes. Figure 10 is a plot of the spectral density for the flapwise bending moment at station 630 (75% span) for data case #2; it shows similar trends but lower overall spectral energy, as expected.

To estimate the contribution to the variance of the flapwise bending moment from various frequency bands, the area under the auto-spectral density plots was calculated in six frequency ranges. Figure 7 shows the low-frequency band and five bands centered about the first five multiples of the rotor speed. The area in each band is the contribution to the signal variance in that frequency band. A trapezoidal integration rule was used to perform this integration numerically, and the large spikes and steep roll-off in the low-frequency region make the integration subject to error. However, the results provide a reasonable order-of-

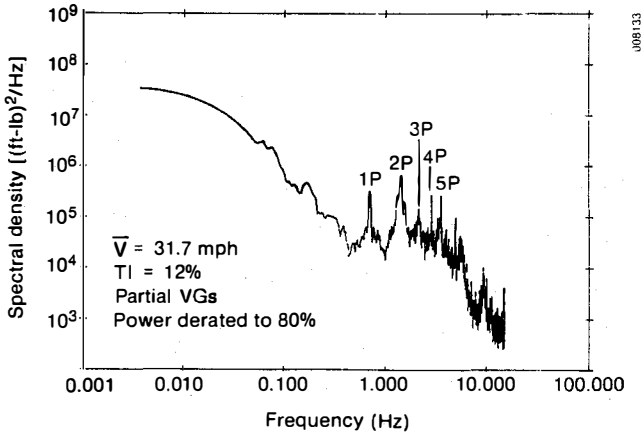

Figure 10. SPECTRAL DENSITY OF THE STATION 630 FLAPWISE BENDING MOMENT FOR DATA CASE #2

magnitude estimate. Table 4 presents the results of these calculations for the flapwise bending moment at blade station 546 for the three data cases. This table clearly shows that the major contribution is from the low-frequency band, although the contributions from all bands is significant when compared with the deterministic loading of Figure 6.

Table 4. VARIANCE CONTRIBUTIONS FOR THE FLAPWISE BENDING MOMENTS AT THE 65% SPANWISE STATION

	$\frac{\sigma^2}{\sigma_T^2}$		
Frequency band	Data case #2	Data case #18	Data case #25
Low-frequency	70%	79%	74%
1P	2%	1%	1%
2P	10%	8%	7%
3P	3%	3%	1%
4P	2%	1%	1%
5P	3%	2%	3%

*σ_T^2 = Total variance of the raw time-series signal.

DISCUSSION

Considering the narrow scope of this quick-look data analysis, the following observations can only be considered tentative (based on a more complete analysis).

1. Energy production, as indicated by Figure 2, appears somewhat better than that advertised; however, much more data, over a wider range of operating conditions, is needed to quantify the actual behavior.

2. The deterministic component of the cyclic loading appears to be quite small when compared to the stochastic component caused by inflow turbulence. This tends to indicate that the teetering hub is operating as expected, and that the rotor is teetering to eliminate much of the loading caused by the mean wind shear in the inflow.

3. The flapwise bending moment at station 546 (65% span) contains broad high-frequency content, showing spikes in the spectral density up through a frequency of 5P. However, the major contribution to the bending-moment variance is from the frequency range below 1P. It should be noted that the turbulence intensity for cases #18 and #25 is quite high (22%-23%), which implies that a major share of the flapping-moment variation is caused by the high turbulence level. This implication will be explored further in later analyses.

The major purpose of this paper was to provide interested researchers and turbine designers with a preliminary look at the test data, as quickly as possible, so that a general impression of the results could be taken into consideration. Field testing was completed in May 1987; since then, the data have been undergoing digitizing, scaling, and reduction. A more complete analysis is expected to take much longer.

REFERENCES

1. Snow, A., and Heberling, C. F., II, Final Report of the Dynamic Loads Tests of the Westinghouse 600 kW Wind Turbine, Draft, Westinghouse Electric Corporation, Pittsburgh, Pennsylvania.

2. Wright, A. D., Buhl, M. L., and Thresher, R. W., FLAP Code Development and Validation, SERI/TR-217-3125, Solar Energy Research Institute, Golden, Colorado, 1987.